Caryologia
International Journal of Cytology, Cytosystematics and Cytogenetics

Firenze University Press
https://riviste.fupress.net/index.php/caryologia

OPEN ACCESS

Citation: Jha, T.B., Halder, M. & Bhowmick, B.K. (2024). Giemsa-based chromosome staining and comparative fluorescent banding pattern in five valuable Indian plant species. *Caryologia* 77(3): 37-45. doi: 10.36253/caryologia-3007

Received: Sep 26, 2024

Accepted: Sep 29, 2024

Published: March 25, 2025

Data Availability Statement: All relevant data are within the paper and its Supporting Information files.

Competing Interests: The Author(s) declare(s) no conflict of interest.

ORCID
TBJ: 0000-0003-0900-8167
MH: 0000-0002-8422-0814
BKB: 0000-0001-6029-1098

Giemsa-based chromosome staining and comparative fluorescent banding pattern in five valuable Indian plant species

Timir Baran Jha[1,*], Mihir Halder[2], Biplab Kumar Bhowmick[3]

[1] *Department of Botany, Maulana Azad College, Rafi Ahmed Kidwi Road, Kolkata-700013, West Bengal, India*
[2] *Department of Botany, Barasat Government College, 10 KNC Road, Barasat, Kolkata-700124, West Bengal, India*
[3] *Department of Botany, Scottish Church College, 1 & 3, Urquhart Square, Manicktala, Azad Hind Bag, Kolkata-700006, West Bengal, India*
*Corresponding author. E-mail: tbjha2000@yahoo.co.in

Abstract. This study presents repeatable enzymatic maceration and air drying (EMA)-based chromosome preparation methods in five valuable Indian plant species namely *Allium cepa*, *Allium sativum*, *Nigella sativa*, *Trigonella foenum-graecum*, and *Aloe vera*. Comparative fluorescent banding studies with two DNA base-specific fluorescent dyes have precisely unraveled the number, position, and patterns of secondary constriction of each species. Additionally, it has highlighted the fluorescent banding pattern of repetitive DNA sequences notably on two important constitutive heterochromatic sites like secondary and primary constrictions. The study has established that EMA-based fluorescent banding can provide valuable complementary information for modern genomics. The results are expected to enrich our knowledge of chromosome biology and crop genomics and inspire future academic and research endeavours.

Keywords: CMA-DAPI banding, Giemsa staining, *Allium cepa* and *Allium sativum, Aloe vera, Nigella sativa, Trigonella foenum-graecum*.

INTRODUCTION

Plants have been serving humanity for centuries. They rely on their species-specific chromosomes not just to carry genetic information, but also for their precise maintenance, management, and transmission (Flavell 2021). Therefore, analyzing and conserving genetic diversity to safeguard their adaptive potential is crucial for valuable populations of wild and domesticated species (Ainsworth 2022) in the era of climatic changes.

Classical cytogenetics has provided foundational information on plant chromosomes for many decades (Guerra 2008; Razumova et al. 2023) in a cost-effective manner. On the other hand, molecular cytogenetics has opened the door to unraveling genetic diversity not only on precise chromosomal morphology but also on the chromosomal DNA composition of

each population and species. Molecular cytogenetics has greatly benefited from the advancement of molecular biology, revealing that chromosomes contain low-copy regulatory gene sequences, while large chunks of DNA are composed of diverse repetitive DNA sequences throughout the length of the chromosomes (Liehr 2021). Some repetitive sequences are well conserved between species, while others define differences even between closely related species. In the 1970s, the introduction of the enzymatic maceration and air-drying (EMA) protocol for plant chromosome preparation (Kurata and Omura 1978), followed by Giemsa staining, and the subsequent application of DNA base-specific fluorochromes in plant chromosome research have helped in individual chromosome identification. These advancements have allowed a profound revision of the structure and function of repetitive DNA patterns in nucleolar organizing regions (NORs), centromeric, subtelomeric, and telomeric regions in many plant species (Fukui et al. 1996; Moscone et al. 1996; Hizume 2015; Jha and Halder 2016; Yamamoto et al. 2019; Jha et al. 2021; Jha and Halder 2023).

Keeping in mind the above-noted considerations the present studies have standardized the EMA-based protocol for chromosome preparation in some valuable Indian species and populations of *Allium cepa* L. (Amaryllidaceae), *Allium sativum* L. (Amaryllidaceae), *Nigella sativa* L. (Ranunculaceae), *Trigonella foenum-graecum* L. (Fabaceae), and *Aloe vera* (L.) Burm. f. (Asphodelaceae). All of these plant species are highly valued for both daily consumption and medicinal purposes. Detailed and comparative chromosomal analysis has been carried out using non-fluorescent Giemsa and two contrasting fluorochromes DAPI (4'-6-diamidino-2-phenylindole) and CMA (chromomycin A3 -CMA) staining. The standardized and repeatable protocol effectively produced numerous cytoplasm-free metaphases and subsequent staining with non-fluorescent and fluorescent dyes, precisely detailed their morphology, and number and positions of secondary constrictions. Additionally, it has highlighted the fluorescent banding pattern of repetitive DNA sequences notably on two important constitutive heterochromatic sites, secondary and primary constrictions. The results of this study are expected to instil interest in students, researchers, and breeders in their future academic and research endeavours, as well as conserve and explore the unique genetic diversity found in other family members of the studied materials.

MATERIAL AND METHODS

Plant materials

The bulbs of two commercially available *Allium* species, *Allium cepa* L. and *Allium sativum* L., were collected and grown in wet sand for 48 hours in the dark. The plants of *Aloe vera* (L.) Burm. f were obtained from a local nursery in Kolkata, West Bengal and grown in the medicinal garden of the Maulana Azad College. The healthy roots of *A. vera* were directly harvested from potted plants. Seeds of *Trigonella foenum-graecum* L. were obtained from the local market, while seeds of *Nigella sativa* L. were collected from a farmer's field in North 24 Parganas, West Bengal, and stored at 4°C. At least 20 seeds of each species were soaked overnight in water, then placed on moist filter paper and kept in the dark at temperatures between 16-22°C for germination. Experimental materials were used several times to harvest roots for chromosome analysis.

Chromosome preparation by enzymatic maceration and air-drying protocol

To standardize the chromosome preparation using the EMA protocol, a minimum of ten healthy root tips measuring 0.7-1 cm in length were collected from germinating seeds, bulbs, or potted plants. Root tips of *A. cepa, A. sativum* and *A. vera* were treated with a saturated solution of Para Dichlorobenzene (PDB), *Trigonella foenum-graecum* with PDB plus Aesculin and *Nigella sativa* with 0.5% Colchicine for 4-5 hours. Fixation was carried out with a 1:3 solution of acetic acid and methanol overnight and then stored at -20°C. The chromosome preparation was carried out following the EMA protocol established by Jha and Halder (2023), with some species-specific minor modifications.

Chromosome staining with Giemsa, DAPI and CMA

The air-dried slides of each species were stained with a phosphate buffer solution containing 2% Giemsa solution (Merck, Germany) for 10-15 minutes to achieve consistent, effective, and optimal staining. After staining, the slides were rinsed three to four times with distilled water air dried with a blower, and finally used for chromosome analysis under a Carl Zeiss compound microscope.

The best Giemsa-stained metaphase slides were destained in 70% methanol for 45 minutes, air-dried and subsequently re-stained with DAPI (0.1-0.2 μg mL^{-1} for 10-15 minutes) and CMA (0.1-0.8 mg mL^{-1} for 70-120 minutes), following Jha et al. (2021) with species-specific modifications.

Chromosome analysis, documentation, and ideogram preparation

A Carl Zeiss AxioLab A1 fluorescence microscope equipped with a CCD camera and computer software was used to examine, documentation, and karyotype analysis of cytoplasm-free metaphase chromosome preparations stained with Giemsa, DAPI, and CMA. Giemsa-stained slides were observed under bright field illumination, while DAPI- and CMA-stained slides were observed under a specific UV filter cassette using the Carl Zeiss Prog Res 2.3.3 software on a computer attached to the microscope. Images of metaphase chromosomes stained with Giemsa, DAPI, or CMA were captured with the help of a CCD camera for analysis.

More than 25 cytoplasm-free mitotic metaphases with well-spread chromosomes displaying distinct karyomorphometric features were chosen for each species. Documentation and measurement of karyomorphometric features such as the lengths of the long and short arms, the positions of the centromeres, the average chromosome length (ACL), the total chromatin length (TCL), and DAPI and CMA signals were performed using Axiovision L.E.4 software. At least five chromosome morphometric data for each species were considered for the calculation of ACL and TCL, and the data was expressed as the mean ± standard deviation (SD). Chromosome nomenclature was based on arm ratios (r = length of long arm/length of short arm) following Levan et al. (1964), and ideograms were prepared by evaluating morphometric data and organizing chromosome pairs in decreasing order of length.

RESULTS

The karyomorphological features of each plant species were determined from cytoplasm free well-spread mitotic metaphases and documented (Figures 1-4, and Table 1-2). Fluorescent staining with DAPI and CMA revealed distinct variability in banding patterns on the chromosomes (Figures 1, 3, Table 2). For the convenience of interpretation, based on the nature of the fluorescent banding pattern, chromosomes were categorized into eight types, namely, type A with CMA^{+ve} (positive) signal in the centromeric region, type B with $DAPI^{+ve}$ signal in the centromeric region, type C with CMA^{+ve} signal at two terminal regions of chromosome, type D with CMA^{+ve} signal at the secondary constriction region, type E with CMA^{+ve} signal at the satellite region and two terminal regions of chromosome, type F CMA^{0} (neutral) / $DAPI^{0}$ (neutral), type G with CMA^{+ve} signals at the centromeric region as well as at the secondary constriction region and type H with $DAPI^{+ve}$ signals at centromeric region and CMA^{+ve} signals in the secondary constriction region (Table 2). It was further confirmed that all CMA^{+ve} bands were $DAPI^{-ve}$ and the $DAPI^{+ve}$ bands were CMA^{-ve}. The unique karyotypes and fluorochrome banding patterns observed in each species are described as follows:

Allium cepa L. (Amaryllidaceae)

The karyotype in *Allium cepa* (2n=16), the age-old model plant material for chromosome studies, revealed the occurrence of five metacentric and three submetacentric pairs of long chromosomes (Fig. 1a-c, Fig. 2a,

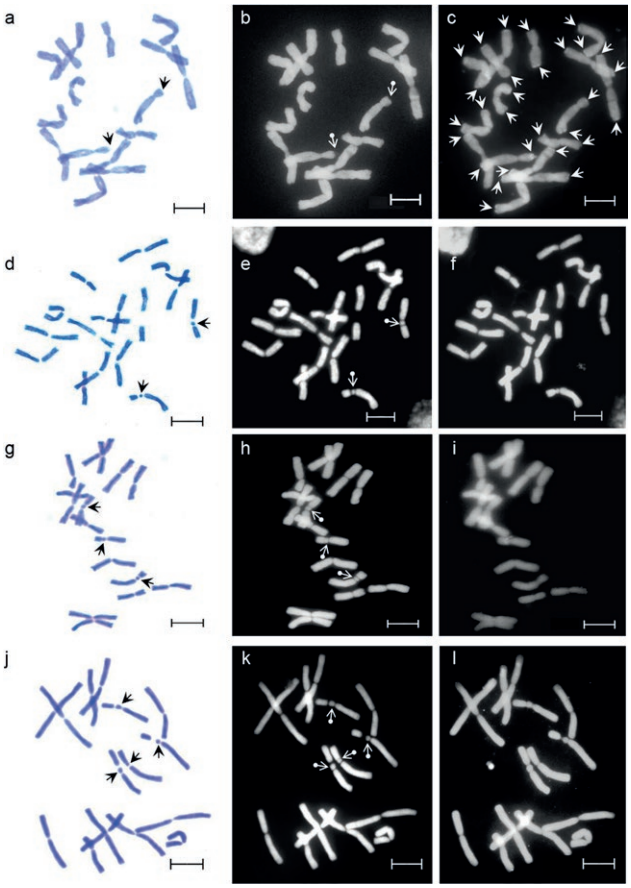

Figure 1. Somatic metaphase chromosomes of *Allium cepa* (2*n*=16) stained correspondingly with Giemsa **(a)**, DAPI **(b)** and CMA **(c)**; Somatic metaphase chromosomes of *Allium sativum* (2*n*=16) stained correspondingly with Giemsa **(d, g, j)**, DAPI **(e, h, k)** and CMA **(f, i, l)**. The positions of two (d-f), three (g-i) and four (j-l) secondary constrictions are indicated with black arrows in Giemsa-stained metaphases and corresponding DAPI negative signals are indicated with white arrows with round end in DAPI-stained metaphases. The positions of terminal CMA positive signals are indicated with white arrows in CMA-stained metaphases. Scale bars=10 μm.

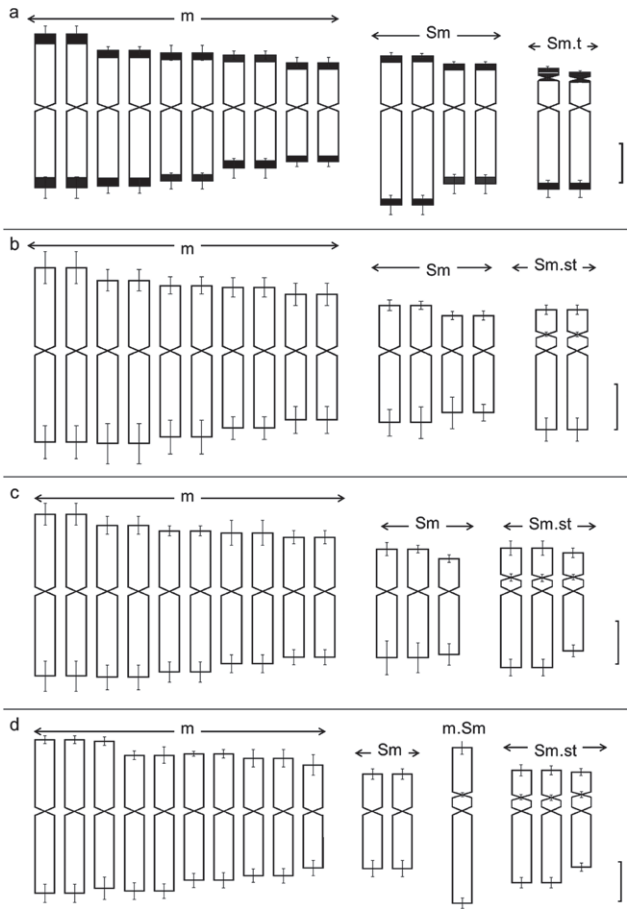

Figure 2. Somatic ideogram of *Allium cepa* (2*n*=16) with two secondary constriction-bearing chromosomes **(a)**; Somatic ideograms of *Allium sativum* (2*n*=16) with two **(b)**, three **(c)** and four **(d)** chromosomes with secondary constrictions. The positions of CMA-positive signals are indicated with black bands. Scale bars=5 μm.

Table 1). Out of three submetacentric pairs of chromosomes, the 6th pair of chromosomes bears the secondary constriction at terminal regions. Screening of over 25 metaphase plates stained with CMA fluorochrome confirmed bright CMA^{+ve} signals at the terminal regions of all chromosomes (Type C, Fig. 1c). Notably, CMA^{+ve} signal was also observed on the satellite of the 6th pair of chromosomes (Type E, Fig. 1c, 2a). Of the one pair of chromosomes with secondary constriction, one of the chromosomes showed a more intense CMA^{+ve} signal on the satellite than the other homologue (Fig. 1c), corresponding with the difference in the size of this satellite in Giemsa-stained chromosomes (Fig. 1a). On the other hand, no AT-specific $DAPI^{+ve}$ signal was observed in any of the chromosomes of this germplasm of *A. cepa* (Fig. 1b). The banding pattern of *A. cepa* thus remains 14C+ 2E with CMA^{+ve} and $DAPI^{-ve}$ signals (Table 2).

Allium sativum L. (Amaryllidaceae)

The studied germplasm of *Allium sativum* L. (Indian garlic) has 2*n* =16 chromosomes (Fig. 1d-l, Table 1), revealing three variant karyotypes with variable numbers (2-4) of chromosomes with secondary constrictions (Fig. 2b-d, Table 2). However, the position of secondary constriction was always interstitial (Fig. 1d-l). The modal karyotype of this species is 10m+4sm+2sm.st (Fig. 2b), with the 6th pair of submetacentric chromosomes exhibiting a secondary constriction region (Fig. 1d). In addition, we have noted three chromosomes with secondary constrictions, i.e. on the 6th pair of both homologous chromosomes plus one chromosome of the 8th pair (Fig. 2c) in some metaphases. Moreover, very few metaphase plates also showed four chromosomes with secondary

Table 1. Karyomorphometric data in the five valuable Indian plant species.

Species (Diploid chromosome number)	CSR in μm (mean±SD)	ACL in μm (Mean±SD)	TCL in μm (mean±SD)	Number of SAT chromosomes (pair number length-wise)	Position of satellite	Diploid Karyotype
Allium cepa (2*n*=16)	10.9±1.20-19.34±2.66	16.93±2.64	241.09±9.85	2 (6th)	T	10m+4sm+2sm.t
Allium sativum (2*n*=16)	8.46±0.71-19.67±2.93	13.54±1.81	224.18±5.85	2 (6th)	I	10m+4sm+2sm.st
				3 (6th, 8th)	I	10m+3sm+3sm.st
				4 (6th, 8th, 1st)	I	10m+2sm+3sm.st+1m.sm
Nigella sativa (2*n*=12)	7.29±0.65-16.64±2.09	13.54±1.81	159.0.9±18.06	6 (2nd, 3rd, 6th)	I	6m+4m.t+2t.sat
Trigonella foenum-graecum (2*n*=16)	8.85±0.76-12.21±1.25	10.34±1.17	165.52±18.42	4 (2nd, 4th)	I	2m+4sm+6st+2m.sm+2m.st
Aloe vera (2*n*=14)	8.52±0.60-30.75±1.08	21.13±10.12	295.86±10.72	4 (1st, 3rd)	T	4st+6sm+4sm.t

CSR: Chromosome size range (range of absolute length of shortest to longest chromosome), ACL: Average length of chromosomes, TCL: Total diploid chromosome length, SAT: Satellite bearing chromosomes, T: Terminal, and I: Interstitial.

constrictions, i.e. on the 6th pair of submedian homologous chromosomes, on one of the 8th pair of submedian chromosomes, and one on the 1st pair of metacentric chromosomes (Fig. 2d; Table 1). Detection of satellite in two heteromorphic and non-homologous chromosomes, i.e., one submedian and one metacentric chromosome, was another interesting finding in this germplasm (Fig. 2d). Interestingly, different karyotype variants were not detected in different metaphases of the same root tip; they were detected in different root tips.

In *A. sativum*, none of the 16 chromosomes showed any CMA^{+ve} or $DAPI^{+ve}$ signals even after repeated trials with varying concentrations of fluorochromes and varying incubation periods. The banding pattern of *A. sativum* thus remains 16F i.e. CMA^{0} / $DAPI^{0}$ (Fig. 1e, f, h, i, k, l, 2b-d, Table 2).

Nigella sativa L. (Ranunculaceae)

The karyotype of *N. sativa* (2n=12) was characterized by one pair of distinctly short telocentric chromosomes and five pairs of long metacentric chromosomes (Fig. 3a-c, Table 1). The secondary constrictions were located on terminal regions of one pair of short chromosomes (6th) and two pairs (2nd and 3rd) of long chromosomes (Fig. 3a, Table 1). The modal karyotype of *N. sativa* was determined as 6m+4m.t+2t.sat (Fig. 4a, Table 1).

CMA-DAPI staining was performed on the same Giemsa-stained metaphase plates to confirm the existence of secondary constrictions in three chromosome pairs (Fig. 3b-c). The staining revealed intense CMA^{+ve} signals at secondary constriction regions that corresponded with $DAPI^{-ve}$ signals (Fig. 3b-c). No additional distinct DAPI/CMA positive/negative signals were found on any chromosomes (Fig. 3b-c) and the fluorochrome banding pattern was determined as 6D+6F (Fig. 4a, Table 2).

Trigonella foenum-graecum L. (Fabaceae)

In *T. foenum-graecum* (2n=16), we have identified the presence of interstitial secondary constrictions at the submetacentric and subtelocentric positions of the 2nd and 4th pairs of chromosomes, respectively (Fig. 3d-f, 4b). The modal karyotype was determined as 6st+4sm+2m+2m.sm+2m.st (Fig. 4b, Table 1). Fluorescent staining revealed very distinct and intense CMA^{+ve} and $DAPI^{-ve}$ signals in all chromosomes at the centromeric regions (Fig. 3e-f). Additionally, the interstitial secondary constriction region of the 2nd and 4th pair of chromosomes also showed CMA^{+ve} and $DAPI^{-ve}$ signals

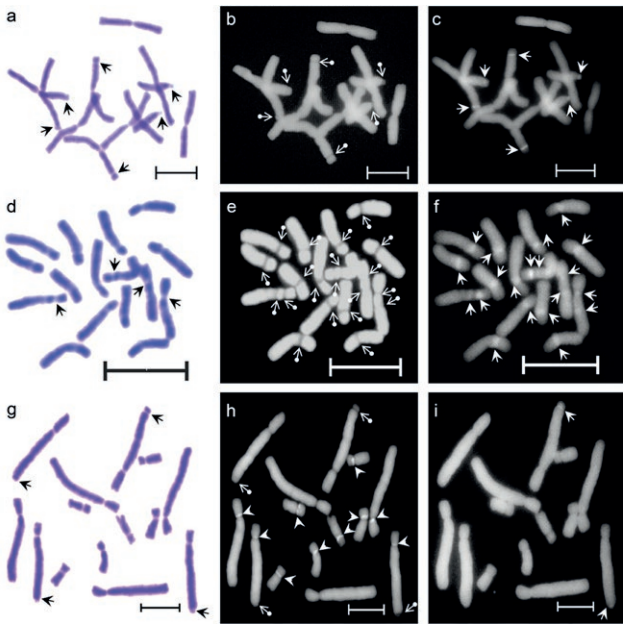

Figure 3. Somatic metaphase chromosomes of *Nigella sativa* (2*n*=12) stained correspondingly with Giemsa **(a)**, DAPI **(b)** and CMA **(c)**; Somatic metaphase chromosomes of *Trigonella foenum-graecum* (2*n*=16) stained correspondingly with Giemsa **(d)**, DAPI **(e)** and CMA **(f)**; Somatic metaphase chromosomes of *Aloe vera* (2*n*=14) stained correspondingly with Giemsa **(g)**, DAPI **(h)** and CMA **(i)**. The positions of secondary constrictions are indicated with black arrows in Giemsa-stained metaphases. DAPI-negative and centromeric DAPI-positive signals are indicated with white arrows with round end and white arrowheads, respectively in DAPI-stained metaphases. CMA-positive signals are indicated with white arrows in CMA-stained metaphases. Scale bars=10 μm.

(Fig. 3e, f, Table 2). The fluorescent banding pattern in *T. foenum-graecum* was 12A+4G (Fig. 4b, Table 2).

Aloe vera (L.) Burm. f. (Asphodelaceae)

The karyotype in *A. vera* (2n=14) consists of three pairs of small (8.52-11.30 μm) submetacentric chromosomes and four pairs of distinctly long (28.26-30.75 μm) chromosomes (Fig. 3g-i, Table 1). The primary constrictions of the long chromosomes were located at the submetacentric or subtelocentric positions, with secondary constrictions at the terminal region of the 1st and 3rd pairs of long chromosomes. (Fig. 3g-i, Table 1).

Fluorescence staining with different concentrations of DAPI and CMA enabled confirmation of chromosomes with secondary constrictions and additional heterochromatic bands in the karyotype. Very faint CMA^{+ve} signals could be seen in two to three chromosomes at their secondary constriction regions (Fig. 3i, Table 2),

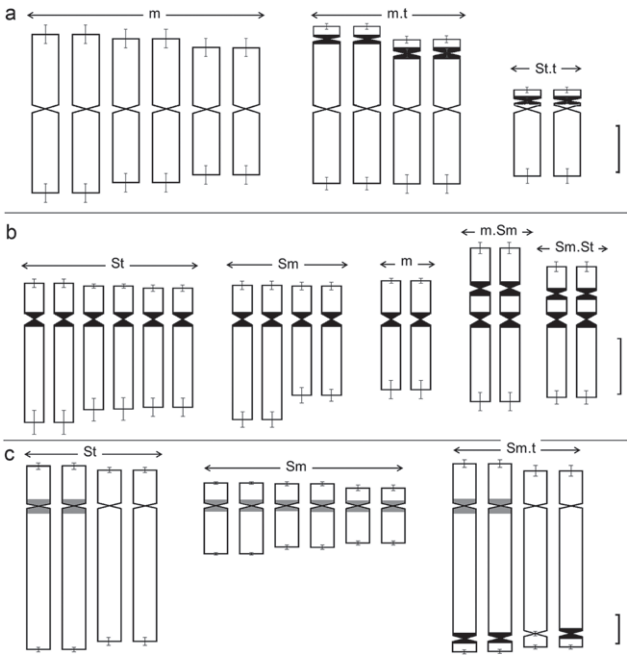

Figure 4. Somatic ideograms of (**a**) *Nigella sativa* (2*n*=12) with six secondary constriction-bearing chromosomes, (**b**) *Trigonella foenum-graecum* (2*n*=16) with four secondary constriction-bearing chromosomes, and (**c**) *Aloe vera* (2*n*=14) with four secondary constriction-bearing chromosomes. The positions of CMA-positive and DAPI-positive signals are indicated with black and grey bands, respectively. Scale bars=5 μm.

corresponding to DAPI^{-ve} signals (Fig. 3h). On the other hand, distinct and intense DAPI^{+ve} signals were scored in all six small chromosomes i.e. in the 5th, 6th and 7th pairs (Fig. 3h, Table 2) and four out of eight long chromosomes. Of these four long chromosomes, one pair had secondary constrictions, and the other was subtelocentric (Fig. 3h, 4c, Table 2). The distinctive CMA-DAPI banding pattern in *A. vera* was 8B+2H+3F+1D (Fig 4c, Table 2).

DISCUSSION

The current research has focused on standardizing chromosome processing using EMA-based preparation and a staining protocol that utilizes both fluorescent and non-fluorescent stains. The fluorescent banding in the species under study has revealed many new features, particularly in two important constitutive heterochromatic sites: secondary and primary constrictions. Both of these sites are considered to be evolutionarily conserved with diverse functions. There are very few comparative fluorescent banding studies available on seemingly common but highly valued plants.

In a standard karyotype of any plant species, the nucleolus organizer region (NOR) acts as a chromosomal marker for researchers and breeders. Guerra (2000) noted that secondary constriction regions are generally GC-rich and display CMA^{+ve} signals. The number and position of secondary constriction regions in the studied materials following the preparation of chromosomes through classical cytogenetics is still a topic of debate (Sato 1980, 1981; Agarwal 1983; Das et al. 2001; Ghosh and Dutta 2006; Das et al. 2011; Martin et al. 2011; Najafi et al. 2013; Shaker et al. 2017). The present investigation confirms the number and positions of secondary constrictions in all the studied species (Table

Table 2. Fluorescent banding patterns in the five valuable Indian plant species.

Species (diploid chromosome number)	Fluorescent banding patterns				Total number of fluorescent signals (CMA^{+ve} + DAPI^{-ve})	Banding pattern
	Chromosome number (p: pair/ s: single)	Position of the signals	Type of signals	Number of signals		
Allium cepa (2*n*=16)	1-8th (p)	Terminal region	CMA^{+}	32	34	14C+2E
	6th (p)	Satellite region	CMA^{+}	2		
Allium sativum (2*n*=16)	1st (s), 6th (p), 8th (s)	Secondary constriction region	CMA^{0} DAPI^{0}	Nil	Nil	16F
Nigella sativa (2*n*=12)	2nd, 3rd, 6th (p)	Secondary constriction region	CMA^{+}	6	6	6D+6F
Trigonella foenum-graecum (2*n*=16)	2nd, 4th (p)	Secondary constriction region	CMA^{+}	4	20	12A+4G
	1-8th (p)	Centromeric region	CMA^{+}	16		
Aloe vera (2*n*=14)	1st (p), 4-7th (p)	Centromeric region	DAPI^{+}	10	12-13	8B+2H+3F+1D
	1st (p), 3rd (s)	Secondary constriction region	faint CMA^{+}	2-3		

Fluorescent banding types- A: CMA-positive centromeric region, B: DAPI-positive centromeric region, C: CMA-positive terminal regions, D: CMA-positive secondary constriction region, E: CMA-positive terminal and secondary constriction regions, F: CMA- neutral and DAPI-neutral, G: CMA-positive centromeric and secondary constriction regions, H: DAPI-positive centromeric region and CMA-positive secondary constriction region.

1). In *Allium cepa* and *Allium sativum*, distinct differences in the number of chromosomes bearing secondary constrictions and fluorescent banding patterns were noted. In *A. cepa*, we scored 34 CMA^{+ve} signals including a pair of chromosomes with a CMA^{+ve} satellite region (Fig. 1b-c, Table 2). In this Indian germplasm, we report heteromorphy concerning $CMA^{+ve}/DAPI^{-ve}$ (GC-rich) band intensity or size in the 6th pair of chromosomes with satellite. Our results conform to Cortes et al. (1983) and Mancia et al. (2015) who have reported terminal bands in all the chromosomes of *A. cepa* through their C-banding and dual colour FISH studies, respectively.

The genus *Allium* has a history of possible chromosome rearrangements related to the distal and interstitial location of NORs in subgenera *Cepa* and *Allium*, respectively (Bhowmick et al. 2023). Numerical variations of secondary constrictions (2-6) have been reported in *A. sativum* (Sato et al. 1980; Cortes et al. 1983; Wajahatullah and Vahidy 1990). But for the first time, we report two to four interstitial secondary constrictions (Fig. 1d-l, Fig. 2b-d) in the Indian germplasm. In *A. sativum*, no CMA and DAPI-positive bands were observed in any chromosomes. It has been reported that chromosomal CMA bands are generally limited for *A. sativum* (Maragheh et al. 2019; Bacelar et al. 2021). However, C-bands were reported in some chromosome pairs of *A. sativum* (Cortes et al. 1983; Yuzbasioglu 2004). The atypical DNA banding pattern in general especially of the secondary constriction regions in *A. sativum* warrants further molecular analyses to unravel the structural complexity and uniqueness.

The use of EMA-based chromosome processing and differential staining has confirmed the presence of three pairs of secondary constrictions for the first time in *Nigella sativa*. Our findings are consistent with the 45S rDNA-loci analysis conducted by Orooji et al. (2022) in a different germplasm of *N. sativa*. However, the observed variation in CMA staining intensity in the NOR regions needs to be addressed in the future at the DNA sequence level. While, in *Trigonella foenum-graecum*, fluorescent banding studies confirmed the presence of two pairs of interstitial secondary constrictions on the 2nd and 4th chromosome pairs. Similar results have been observed in other germplasms through fluorescent banding and rDNA hybridization studies (Ahmad et al. 1999; Santra et al. 2023). Fluorescent banding studies in *Aloe vera* reveal secondary constrictions at the terminal region of 1st and 3rd pairs of long chromosomes (Table 2). However, $CMA^{+ve}/DAPI^{-ve}$ signals were obtained distinctly in one pair of secondary constricted chromosomes and the other pair remains indistinct and difficult to determine in many metaphases. Adams et al. (2000) reported variability in rDNA sites within the genus *Aloe* and reported three pairs of rDNA sites in *A. vera*.

In comparative studies of centromeric sites, three types of DNA sequence organization have been observed in the studied species: $CMA^{+ve}/DAPI^{-ve}$ (GC rich), $DAPI^{+ve}/CMA^{-ve}$ (AT-rich), and $CMA^{0}/DAPI^{0}$ (GC-AT neutral). CMA^{+ve} centromeric sites have not been reported in many plant species. Mondin et al. (2011) reported it in *Crotalaria juncea* (2n=16). Than et al. (2017) reported CMA^{+ve} centromeric sites in all the chromosomes of *Swertia nervosa* (2n=26), only in one pair in *S. chirayita* (2n=26), but not a single centromeric region of *S. bimaculata* (2n=26) chromosomes. In *Trigonella*, intense CMA^{+ve} signals have been found in the centromeric regions of all chromosomes in the present study. A similar report has been published by Santra et al. (2023) in *Trigonella*. Further fluorescent banding studies in different plant species are required to unravel DNA sequence patterns. Further fluorescent banding studies in *Trigonella* species and populations are equally necessary to confirm whether the CMA^{+ve} GC-rich centromeric nature is global or local in *Trigonella*.

On the other hand, a well-established bimodal karyotype in *Aloe vera* with eight long and six small chromosomes (2n=14) showing unique $DAPI^{+ve}/CMA^{-ve}$ fluorescent banding patterns in all six small and four long chromosomes is reported for the first time in this species. It is recognized that the centromere in every eukaryotic chromosome is a multifunctional dynamic complex. Despite mediating the evolutionarily conserved function of directing chromosome segregation, they show surprising diversity in their DNA sequence organisation (Tong et al. 2019; Barbosa et al. 2022). DNA sequence analysis in rice, maize, and *Arabidopsis* has shown that centromeres are composed of highly repetitive DNA sequences with considerable size variation and sequence divergence (Ma et al. 2007) but rarely has it been characterized as GC- or AT-rich or GC–AT neutral regions. On the other hand, the fluorescent banding patterns directly observed on the metaphases in highly conserved centromeric sites of *Trigonella, Aloe, Nigella* and *Allium* revealed their contrasting species and even chromosome-specific DNA divergence and necessitate further fluorescent banding and DNA sequencing studies in the future. We encourage further analysis of fluorescent banding in other plant species to gain a better understanding of the nature of DNA organization in secondary and centromeric regions. We hope that our findings will inspire researchers and scientists to come up with new ideas for studying chromosomes in plants.

CONCLUSION

The use of a repeatable EMA-based protocol for comparative fluorescent banding can be applied to any plant species with minor modifications. Recent studies on five common but valuable plant species have provided interesting and thought-provoking information on the nature of repetitive DNA sequences in two constitutive heterochromatin sites directly on the metaphase plates. The research has shown that EMA-based fluorescent banding can offer valuable complementary information for modern genomics. The results are expected to enhance our understanding of chromosome biology and crop genomics and to inspire future academic and research endeavours.

ACKNOWLEDGEMENTS

In honour of his mentor and teacher, the late Prof. A. K. Sharma, TBJ dedicates this paper to his birth centenary year. He would like to acknowledge Dr S. Dutta, the Principal, and Dr D. Mukhopadhya, the Head of the Department of Botany at Maulana Azad College, for providing basic facilities. MH expresses gratitude to the Principal of Barasat Government College, Kolkata, for his active support and encouragement in research activities. BKB is thankful to the Principal of Scottish Church College for encouraging research activities.

REFERENCES

Adams SP, Leitch IJ, Bennett MD, Chase MW, Leitch AR. 2000. Ribosomal DNA evolution and phylogeny in *Aloe* (Asphodelaceae). Ame J Bot. 87(11): 1578–1583.

Agarwal K. 1983. Cytological studies in the genus *Trigonella* Linn. Cytologia 48(4):771–779. https://doi.org/10.1508/cytologia.48.771

Ahmad F, Acharya SN, Mir Z, Mir PS. 1999. Localization and activity of rRNA genes on fenugreek (*Trigonella foenum-graecum* L.) chromosomes by fluorescent in situ hybridization and silver staining. Theor Appl Genet. 98:179–185. https://doi.org/10.1007/s001220051056

Ainsworth D. 2022. UN convention on biological diversity (COP 15) held in Montreal Canada.

Bacelar PAA, Feitoza LL, Valente SES, Gomes RLF, Martins LV, Almeida PM, Silva VB, Lopes ACA, Carvalh R, Peron AP. 2021. Variations in heterochromatin content reveal important polymorphisms for studies of genetic improvement in garlic (*Allium sativum* L.). Braz J Biol. 83: e243514. https://doi.org/10.1590/1519-6984.243514

Barbosa AC, Xu Z, Karari K, Williams W, Hauf S, Brown WR. 2022. Mutation and selection explain why many eukaryotic centromeric DNA sequences are often A+ T rich. Nu Acid Res. 50(1):579–596. https://doi.org/10.1093/nar/gkab1219

Bhowmick BK, Sarkar S, Roychowdhury D, Patil SD, Lekhak MM, Ohri D, Rao SR, Yadav SR, Verma RC, Dhar MK, Raina SN. 2023. *Allium* cytogenetics: a critical review on the Indian taxa. Comp Cytogenet. 17:129. 10.3897/CompCytogen.17.98903

Cortes F, Gonzalez-Gil G, Hazen MJ. 1983. C-banding and sister chromatid exchanges in three species of the genus *Allium* (*A. cepa*, *A. ascalonicum* and *A. sativum*). Caryologia 36(3):203–210. https://doi.org/10.1080/00087114.1983.10797661

Das A, Mukherjee P, Ghoroi A, Jha TB. 2011. Comparative karyomorphologycal analyses of *in vivo* and *in vitro* grown plants of *Aloe vera* l. Burm. F. Nucleus 53(3):89–94.

Das AB, Mohanty S, Das P. 2001. Cytophotometric estimation of 4C DNA content and karyotype analysis in ten cultivars of *Trigonella foenum-graecum*. Iran J Bot. 9(1):1–9

Flavell RB. 2021. Perspective: 50 years of plant chromosome biology. Plant Physiol. 185(3):731-53. https://doi.org/10.1093/plphys/kiaa108

Fukui K. 1996. Plant chromosomes at mitosis. In: Fukui K, Nakayama S, editors. Plant chromosomes: laboratory methods. Boca Raton (BR): CRC Press; p. 1–17.

Ghosh A, Datta AK. 2006. Karyotyping of *Nigella sativa* L. (black cumin) and *Nigella damascena* L. (love-in-a-mist) by image analyzing system. Cytologia 71(1):1–4.

Guerra M, Santos KGBD, Silva AEB, Ehrendorfer F. 2000. Heterochromatin banding patterns in Rutaceae-Aurantioideae– a case of parallel chromosomal evolution. Am J Bot. 87(5):735–747. https://doi.org/10.1159/000121083

Guerra M. 2008. Chromosome numbers in plant cytotaxonomy: concepts and implications. Cytogenet Genom Res. 120(3–4):339–350.

Hizume M. 2015. Fluorescent banding pattern in chromosomes of *Tsuga forrestii* and *T. Sieboldii* Pinaceae. Chromo Bot. 10(3):95–100. https://doi.org/10.3199/iscb.10.95

Jha TB, Bhowmick BK, Roy P. 2021. Analysis of CMA-DAPI bands and preparation of fluorescent karyotypes in thirty Indian cultivars of *Lens culinaris.* Caryologia 74(2):65–77.

Jha TB, Halder M. 2016. Searching chromosomal landmarks in Indian Lentils through EMA-based Giemsa staining method. Protoplasma 253:1223–1231.

Jha TB, Halder M. 2023. Evaluation of karyotype diversity in Indian traditional aromatic rice cultivars through EMA-based non-fluorescent Giemsa and fluorescent DAPI staining. Genet Resour Crop Evol. 1–22. https://doi.org/10.1007/s10722-023-01696-4

Kurata N, Omura T. 1978. Karyotype analysis in rice I. A new method for identifying all chromosome pairs. Jpn J Genet. 54:251–255. https://doi.org/10.1266/jjg.53.251

Levan A, Fredga K, Sandberg AA. 1964. Nomenclature for centromeric position on chromosomes. Hereditus. 52:210–220.

Liehr T. 2021. Molecular cytogenetics in the era of chromosomics and cytogenomic approaches. Front Genet. 12:720507.

Ma J, Wing RA, Bennetzen JL, Jackson SA. 2007. Plant centromere organization: a dynamic structure with conserved functions. Trends Genet 23(3):134-139.

Mancia FH, Sohn SH, Ahn YK, Kim DS, Kim JS, Kwon YS, Kim CW, Lee TH, Hwang YJ. 2015. Distribution of various types of repetitive DNAs in *Allium cepa* L. based on dual-colour FISH. Hortic Environ Biotechnol. 56(6):793–799. https://doi.org/10.1007/s13580-015-1100-3

Maragheh FP, Janus D, Senderowicz M, Haliloglu K, Kolano B. 2019. Karyotype analysis of eight cultivated *Allium* species. J Appl Genet. 60(1):1–11. https://doi.org/10.1007/s13353-018-0474-1

Martin E, Akan H. Ekici M, Aytac Z. 2011. Karyotype analyses of ten sections of *Trigonella* (Fabaceae). Comp Cytogenet. 5(2):105. 10.3897/compcytogen.v5i2.969

Mondin M, Aguiar-Perecin ML. 2011. Heterochromatin patterns and ribosomal DNA loci distribution in diploid and polyploid *Crotalaria* species (Leguminosae, Papilionoideae), and inferences on karyotype evolution. Genome 54:718–726. https://doi.org/10.1139/g11-034

Moscone EA, Lambrou M, Ehrendorfer F. 1996. Fluorescent chromosome banding in the cultivated species of *Capsicum* (Solanaceae). Plant Syst Evol. 202:37–63. https://doi.org/10.1007/BF00985817

Najafi S, Anakhatoon EZ, Birsin MA. 2013. Karyotype characterisation of reputed variety of fenugreek (*Trigonella foenum-graecum*) in West Azerbaijan-Iran. J Appl Biol Sci. 7(1):23–26.

Orooji F, Mirzaghaderi G, Kuo YT, Fuchs J. 2022. Variation in the number and position of rDNA loci contributes to the diversification and speciation in *Nigella* (Ranunculaceae). Front Plant Sci. 13:917310. https://doi.org/10.3389/fpls.2022.917310

Razumova OV, Alexandrov OS, Bone KD, Karlov GI, Divashuk MG. 2023. Sex chromosomes and sex determination in dioecious agricultural plants. Agron 13(2):540. https://doi.org/10.3390/agronomy13020540

Santra I, Biswas D, Ghosh B. 2023. Chromosomal characterization mediated by karyomorphological analysis and differential banding pattern in fenugreek (*Trigonella foenum-graecum* L.): a neglected legume. Caryologia 76(3):63–70. https://doi.org/10.36253/caryologia-2159

Sato S, Hizume M, Kawamura S. 1980. Relationship between secondary constrictions and nucleolus organizing regions in *Allium sativum* chromosomes. Protoplasma 105:77–85. https://doi.org/10.1007/BF01279851

Sato S. 1981. Cytological studies on the satellited chromosomes of *Allium cepa*. Caryologia 34(4):431–440. https://doi.org/10.1080/00087114.1981.10796911

Shaker SS, Mohammadi A, Shahli MK. 2017. Cytological studies on some ecotypes of *Nigella sativa* L. in Iran. Cytologia 82(2):123–126. https://doi.org/10.1508/cytologia.82.123

Than MMM, Samaddar T, Bhowmick BK, Jha S. 2017. Fluorescent chromosome banding and genome size estimation in three species of Swertia. Cytologia 82(5):513–520.

Tong P, Pidoux AL, Toda NR, Ard R, Berger H, Shukla M, Torres-Garcia J, Müller CA, Nieduszynski CA, Allshire RC. 2019. Interspecies conservation of organisation and function between nonhomologous regional centromeres. Nat Commun. 10(1):2343. https://doi.org/10.1038/s41467-019-09824-4

Wajahatullah MK, Vahidy AA. 1990. Karyotyping and localization of nucleolar organizer regions in Garlic, *Allium sativum* L. Cytologia. 55(3):501–504. https://doi.org/10.1508/cytologia.55.501

Yamamoto M, Takeuchi M, Nashima K, Yamamoto T. 2019. Enzyme maceration, fluorescent staining, and FISH of rDNA of Pineapple (*Ananas comosus* (L.) Merr.) chromosomes. J Hortic. 88(4):455–461.

Yuzbasioglu D. 2004. Karyotyping, C- and NOR banding of *Allium sativum* L. (Liliaceae) cultivated in Turkey. Pak J Bot. 36(2):343–349.